

Phase states in amorphous carbon*

A.S.Bakai, Yu.A.Turkin and M.P.Fateev

NSC Kharkov Institute of Physics and Technology, Akademichna 1, 61108 Kharkov, Ukraine

April 26, 2024

Abstract

Amorphous carbon (a-C) formed under energetic atom deposition and by cooling of a melt by MD simulations in a wide P, T -range is investigated. Simulations of a-C formation with atomic beam deposition reveal a sharp GLC-to-DLC transition with $z = 3.35$. The average coordination number, z , depends on the depositing atom energy. Voronoi polyhedra of the 3-coordinated atoms changes dramatically in the vicinity of the transition while for the 4-coordinated atoms they are changing a few. The elastic moduli along with densities of states of electrons and phonons in the GLC and DLC states are investigated. Changes of a-C with temperature and pressure evolution and GLC-DLC transformations are studied. The map of isoconfigurational states on the (P, T) -plane shows regions of GLC and DLC phases stability.

arXiv:cond-mat/0108518v1 30 Aug 2001

*to be published in *Nanostructured Carbon for Advanced Application*, 185-198, ed. G. Benedek et al. (2001 Kluwer Academic Publisher, Netherlands).

1 Introduction

Amorphous carbon (a-C) in solid state is a rather big family of carbon materials with many types of short-range and medium-range orders (SRO and MRO). From thermodynamic point of view any a-C is a non-ergodic and non-equilibrium system. The diffusional structure relaxation time in graphite and diamond at $T < 10^3$ K is huge because the activation energy of this process is estimated to be larger than 7 eV. In a-C the structure relaxation processes are also very slow at those temperatures. Therefore many forms of a-C are rather stable to be used and investigated. Structure of solid a-C is a continuous random network (CRN). The local order (LO) of an atom is determined by configuration of its covalently bonded nearest neighbors. Because of polyvalence the a-C network possesses an alternating LO. The topologic disorder of the network originates from both alternating LO and random local distortions. The MRO of CRN is mainly determined by correlations of atoms of the same LO and by orientational correlation of the Voronoi polyhedra. From general point of view there are no restrictions on the ratios c_2/c_3 and c_3/c_4 (c_2, c_3, c_4 are concentrations of sp -, sp^2 -, sp^3 - fractions), as well as on the range and characteristics of MRO. The structure properties of a-C are determined by kinetics of its formation. For this reason different forms of a-C are characterized by the initial (essentially non-equilibrium) state of C and by the method of its preparation. Here we are concentrated on investigations of topology and properties of a-C obtained by atom (ion) beam deposition and by modelling of cooling of a melt in a wide P, T -range. These forms of a-C have a lot of applications [1-4]. Experimental information concerning the microscopic structure of these materials is incomplete, but big variety of their macroscopic properties is observed. In [2] the a-C films were separated on the graphite-like (GLC) and diamond-like (DLC) rather qualitatively: those films which have macroscopic properties (density, hardness, electric and heat conductivity) similar to that of diamond are treated as DLC. Otherwise the films are GLC. It was believed [4] that mainly the big concentration of sp^3 bonding is responsible for the diamond-like properties. Meanwhile computer simulations [5] showed up that the distorted sp^2 -network with low sp^3 fraction can have diamond-like macroscopic properties. It was still unclear whether there are topological and thermodynamic criteria of the GLC and DLC state classification. The canonical thermodynamic approach is not valid in the case of a non-ergodic system [6]. Therefore we start from the polyamorphizm problem formulation. Then molecular dynamic (MD) computer simulations are used to get an answer whether the polyamorphous states of a-C (GLC and DLC) can be identified or not. It turns out that the positive answer does exist at least in the case of a-C with Tersoff's or Brenner's classic empiric potential. The classical empiric potential simulations (CEPS) of a-C formation with atomic beam deposition reveal that a sharp GLC-to-DLC transition takes place with $z = z^* = 3.32$, z is the average coordination number of a-C. It depends on the depositing atom energy, E_a . We have compared the densities of states (DOS) of electrons and phonons in the GLC and DLC states. To calculate them the tight-binding MD (TBMD) simulations were performed.

Further changes of a-C with temperature and pressure evolution and GLC-to-DLC transformations in the CEPS are investigated. The map of isoconfigurational states on the (P, T)-plane shows regions of GLC and DLC phase stability. Specific volume and potential energy of a-C as functions of P, T along with the map of isoconfigurational states allow to determine glass-to-liquid transition temperature, T_g , vs P . In result the phase diagram of a-C is constructed. It has to be pointed out from very beginning that all of the obtained results concern the model a-C with the chosen classical empiric potential or with the TB interactions. Nevertheless we believe that they mimic reality at least qualitatively.

2 Polyamorphizm of a-C

The term "polyamorphizm" was introduced in analogy with "polymorphizm" in [7] and then was reintroduced independently by others [8]. Literally it means that a system can exist in two different amorphous phase states of the same composition. Concerning solid amorphous states the given definition became invalid because many non-ergodic structure states with different structure and thermodynamic properties can be stable at the same (P, T)-point for much longer than the observation time. Moreover the number of the possible structure states is exponentially large (see below). Therefore the free energy has a lot of comparable minima in the phase space (see e.g. [8, 9]). The minima set can be ordered by the following way. A subset of the minima of a comparable depth which are separated by low barriers and correspond to states of different SRO's forms a basin of the structure states. The basins are separated by higher barriers. Those basins which have comparable depths and similar structure properties of states within

them do form megabasins [8]. The number of structure states within of a megabasin is determined by configurational entropy or complexity [6], ζ_i (i is the index numbering the megabasins):

$$W(N) = \exp(\zeta_i N) + W_{ne}(N) \quad (1)$$

Here N is the number of atoms and W_{ne} is the number of the structure states which do not contribute into the configurational entropy in thermodynamic limit,

$$\lim_{N \rightarrow \infty} \ln W_{ne}/N = 0 \quad (2)$$

Transitions within a basin are governed by the short range atomic rearrangements. The characteristic time of these rearrangements, τ_{SRO} , is the shortest of the structure transformation times. MRO transformation needs correlated structure rearrangements which can be connected with formation of stressed regions or inner boundaries. This process needs also the short range diffusion. The characteristic time of this transformation, τ_{MRO} , as a rule, is much longer as compare with τ_{SRO} . The long-range ordering time, τ_{LRO} , is the largest of the structure relaxation times. The observation time, t_{obs} , has to be much shorter than τ_{LRO} , otherwise a stable crystalline phase forms. The averaged within i -th megabasin free energy, $\langle G_i \rangle$, depends on P, T . It is the thermodynamic quantity which characterized the amorphous phase and makes understandable the polyamorphism thermodynamics. The difference

$$\Delta G_{ij} = \langle G_i \rangle - \langle G_j \rangle \quad (3)$$

determines stability of the amorphous phases. Crossover of the ‘‘coexisting curve’’,

$$\Delta G_{ij}(T, P) = 0, \quad (4)$$

is the necessary condition of the polyamorphic transformation. Let us denote by $T_{12}(P)$ the coexistence temperature of phase states 1 and 2. The transformation is observable with

$$\tau_{LRO} \gg t_{obs} \gg \tau_{SRO}^{12} \quad (5)$$

or

$$\tau_{LRO} \gg t_{obs} \gg \tau_{MRO}^{12} \quad (6)$$

Here $\tau_{SRO}^{12}, \tau_{MRO}^{12}$, are times of transition from a state within the megabasin 1 into a state within the megabasin 2. Because of the multiplicity of the structure states within the basins, (1), one can expect that the polyamorphic transformation in result of a sequence of the short range rearrangements is possible and the condition (5) is satisfiable. In the case of a-C it seems that this condition can be fulfilled at least for polyamorphic states which differ mainly by LO. MD simulations mimic the kinetics of the structure formation evolution. The time of state1 to state2 transformation which controlled by the short-range rearrangements can be presented in the following form

$$\tau_{SRO}^{12} = \tau_{SRO}^0 \sinh(\Delta G_{12}\beta) = \nu_0^{-1} \exp(-h_{SRO}\beta) \sinh(\Delta G_{12}\beta) \quad (7)$$

where $\beta \equiv 1/k_B T$, k_B is the Boltzmann’s constant; ν_0 is the frequency of ‘‘attempts’’ (it is about the Debye frequency); h_{SRO} is the activation enthalpy of the short-range rearrangements. ΔG_{12} , the difference of the free energies of the states, is the thermodynamic driving force of the transformation. This expression is valid with $\Delta G_{12}\beta \ll 1$. The essential difference of the specific volumes, compressibilities and thermal expansion coefficient of graphite and diamond allows to expect that these quantities along with c_2, c_3, c_4 are enough to identify GLC and DLC.

3 Topologic transition in a-C deposited from atom beam

We have performed the CEPS (with Tersoff’s potential) of a-C deposited from atom beam. The structure and properties of the obtained ‘‘samples’’ (with N up to 1800) were investigated. Some results of similar MD simulations of Kaukonen et al. (with $N = 516$) are reported in [10]. These results are confirmed in our investigations but our main goal is the assumed polyamorphism of a-C. Beam deposition on diamond substrate at $T = 300$ K produces low-density and high-density samples (see Fig. 1), dependently of E_a . Density and coordination number, z , vs E_a are shown on Fig. 2. Besides of the dramatic increasing

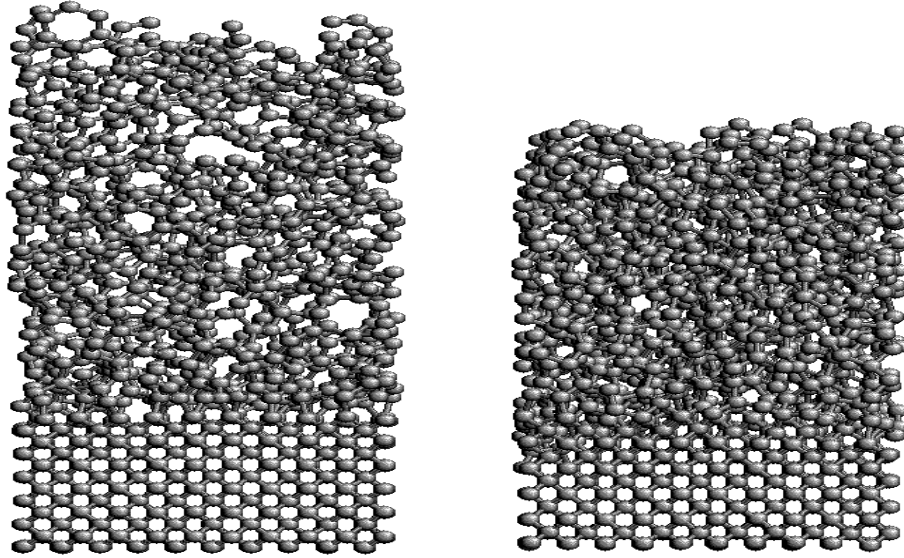


Figure 1: a-C films deposited on diamond substrate from atom beam with energy (a)1 eV, and (b) 40 eV; $N = 1800$

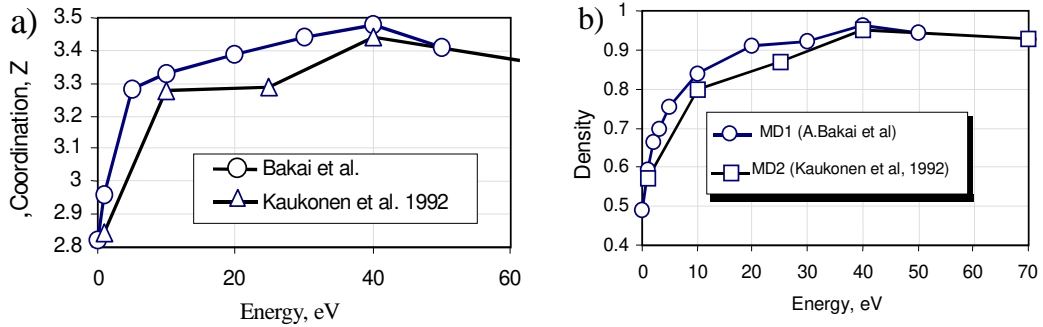


Figure 2: (a)Coordination number, and (b) density (in units of diamond density) as functions of the energy E_a

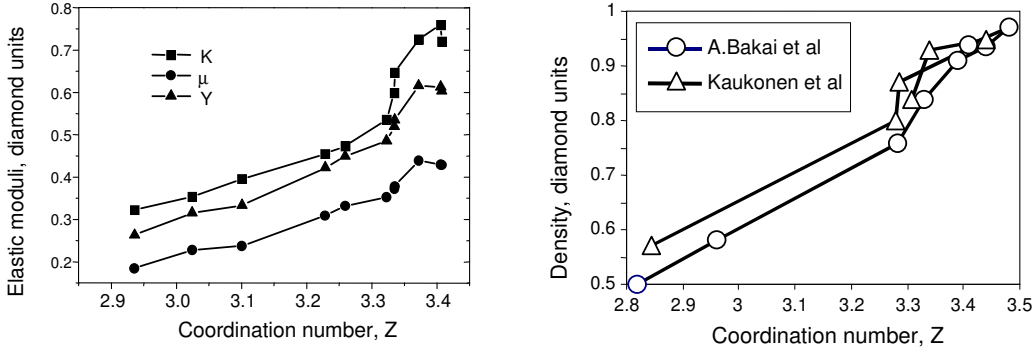


Figure 3: (a) Elastic moduli, and (b) density as functions of the coordination number

of the density at very low $E_a < 10$ eV, no specific behavior of these quantities are observed. Pair correlation function of 3-fold and 4-fold coordinated atoms show that independently of E_a correlations are significant only up to second coordination shell and that average pair correlation radius, r_c , is about 2.5\AA . Apparently, SRO determines properties of this a-C. When the density, and bulk, shear and Young moduli, μ , K and Y are plotted vs z (Fig. 3), all these quantities “jump” up to 30% in the vicinity of $z = z^* = 3.32$. It looks like a phase transition on z . Because the pair correlation functions show up no dramatic changes in the vicinity of z^* it is clear that SRO changes are responsible for the observed singularity.

Voronoi and Deloney divisions (they are dual each to other) are useful in topology investigations. The results of analysis of Voronoi polyhedra are presented on Fig. 4 and Fig. 5. Voronoi polyhedra of 4-fold coordinated atoms are almost unchanged in shape and volume at any z . Voronoi cells of the 3-fold coordinated atoms are distorted three-angled prisms at any z but their volume changes essentially. The Voronoi polyhedra of the 3-fold and 4-fold coordinated atoms at $z > z^*$ are shown on Fig. 4.

At low E_a the average volume of cell of 4-fold coordinated atoms, $v_4 = 6.92\text{\AA}^3$, is something larger than that with $z > z^*$, ($v_4 = 5.74\text{\AA}^3$, due to contribution of micropores in the former case. Note that $v_4 = 5.63\text{\AA}^3$ for diamond at $T \rightarrow 0$. The specific volume of 3-fold coordinated atoms dramatically depends on E_a . It is equal to 9.26\AA^3 at $z < z^*$ and to 6.68\AA^3 with $z > z^*$. Remarkably that the specific volumes of both 3-fold and 4-fold coordinated atoms do not depend on z (or density) with $z > z^*$ (5). One could say that 6.68\AA^3 is close to a quantum limit of 3-fold coordinated carbon. The specific volume of graphite, $v_3 = 9\text{\AA}^3$ at $T = 0$, is far above this limit. It is worth noticing that the calculated v_3 of a-C at is close to specific volumes of some stable graphens with large distortions of the sp^2 -network. In onions the interlayer distance for inner layers is about 2.2\AA and average volume per atom is about 6\AA^3 . A similar estimation can be obtained for the volume per atom within inner tubes of multi-wall nanotubes. In [5] the quenched glassy carbon of high density, ($3.2\text{ g/cm}^3, z = 3.8$) in result of relaxation at $T = 1500\text{ K}$ transforms into stable a-C with $c_3 = 0.75, c_4 = 0.25$ and $\rho = 2.9\text{ g/cm}^3$. No essential changes of z and ρ were observed on the ending stage of the annealing. Kelires has pointed out that the revealed DLC in its nature is a type of GLC because of low c_4 . The estimated specific volume, \bar{v} , in this a-C is $\approx 6.75\text{\AA}^3$ what is in nice harmony with obtained numbers in our simulations. To investigate the densities of states of phonons and electrons a TBMD simulation method was used. Cells of up to $N = 212$ were cut from the prepared in CEPS samples. Afterward the TBMD simulations were performed to provide the structure relaxation and to get the densities of states. It was found a considerable relaxation of the samples on the initial stage of this procedure. The CEPS give more crude simulation than the TBMD method (for details see [11]). Despite changes of density and coordination in result of the relaxation are not so large, changes of the electron and phonon densities of states of the samples in initial states and after relaxation are significant.

On Fig. 6 the electron density of states for as obtained (dashed line) and TBMD-relaxed sample (solid line) with $z < z^*$ and $z > z^*$ are shown. It is seen that the CEPS gives more non-equilibrium configurations and, as a result, a maximum of electron states at Fermi level, E_f , exists. After TBMD-relaxation a pseudogap of about 2 eV width forms around E_f . Very similar electron densities of states

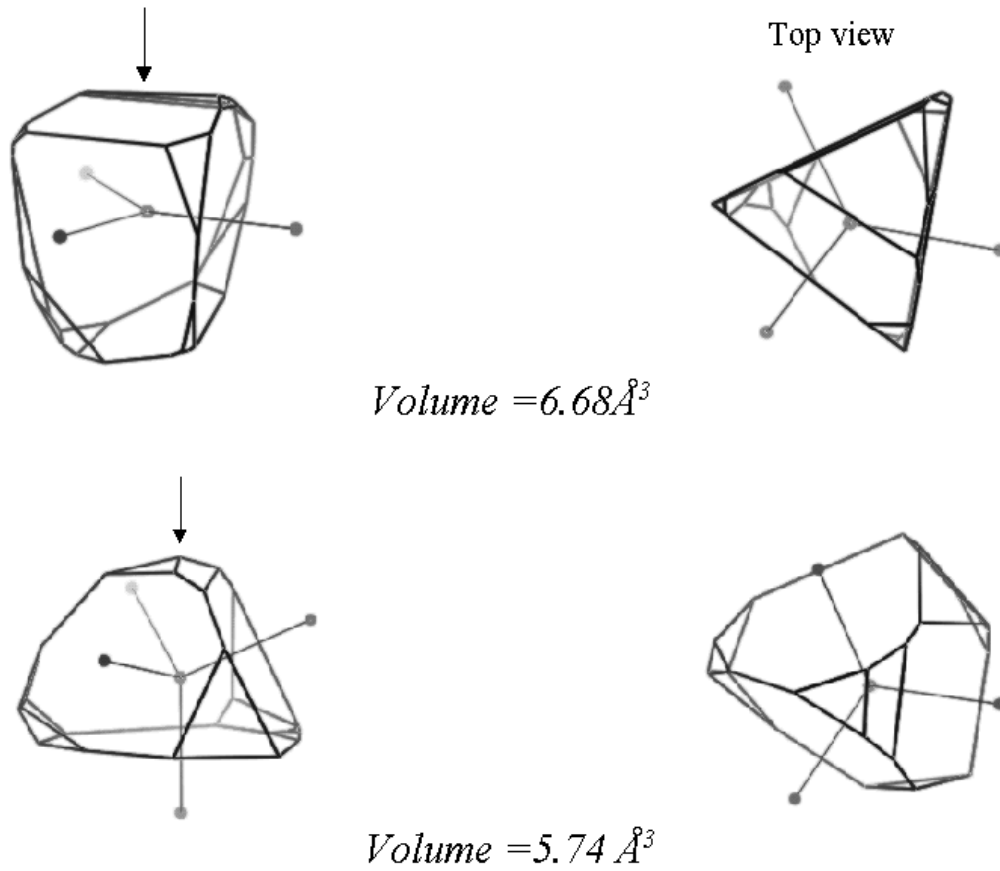


Figure 4: Voronoi polyhedra of film deposited from 40 eV carbon beam

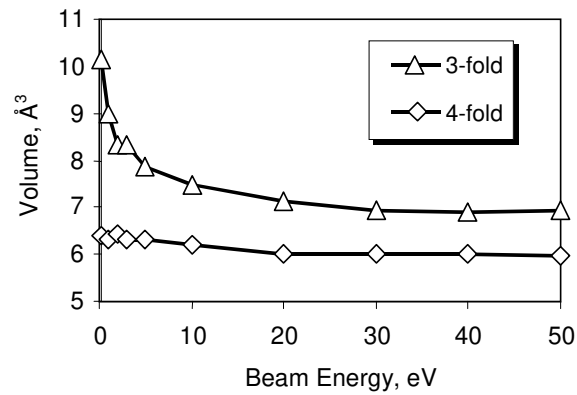


Figure 5: Volumes of Voronoi polyhedra of the 3-fold and 4-fold coordinated atoms vs the beam energy, E_a

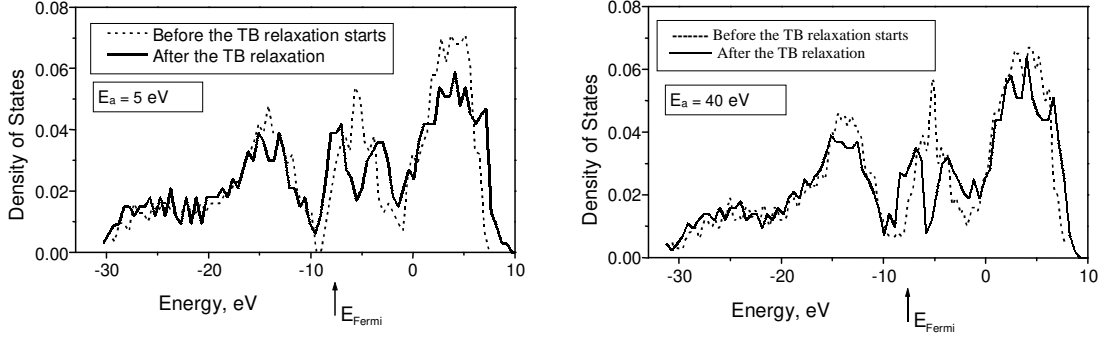


Figure 6: Electron densities of states, TBMD simulations

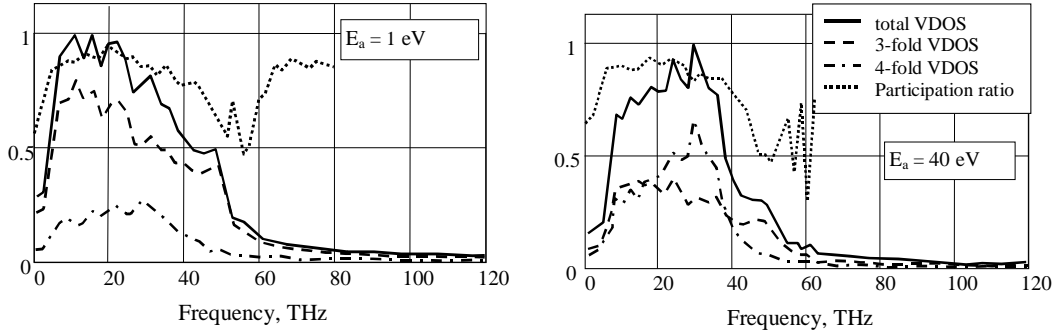


Figure 7: Vibrational densities of states, TBMD simulations

are obtained for a-C in [11-13] in TB and Car-Parinello approaches. A minor difference of the electron densities of states of the structures with $z < z^*$ and $z > z^*$ can be recognized. It means that the shape of π -electron band is not more sensitive to topological disorder when the mobility edge is absent and no extended states do exist. The phonon densities of states are more sensitive to the network local order and topology, because of the changes of the elastic moduli. The participation ratio (dotted lines on Fig. 7) is lower with $z > z^*$ for the high frequency phonons.

(Because the rigidity of a-C is higher with $z > z^*$, the main maximum of the phonon density of states is shifted from $\nu = 10$ THz at $z < z^*$ to $\nu = 30$ THz at $z > z^*$). It means that the localization radius of the high frequency phonons decreases with densification and with increasing distortions around of sp^2 -bonded atoms. It is worth to note that because the size of the simulation cell is not so large ($L < 10a$, a is the average interatomic distance) the calculated participation ratio here is rather a qualitative characteristic of the localization phenomenon. The used atomic beam deposition procedure is based on fast quenching of as deposited atoms. The obtained GLC ($z < z^*$) and DLC ($z > z^*$) have essentially different structures and properties and coexist at the same P, T just because the time of the depositing atom thermalization and t_{obs} are shorter than τ_{SRO} (7). Nevertheless the revealed topological transition in the vicinity of z^* is a good starting point to look for metastable polymorphous states of a-C. For this purpose formation and evolution of a-C under fulfilled condition (5) have to be performed (see below).

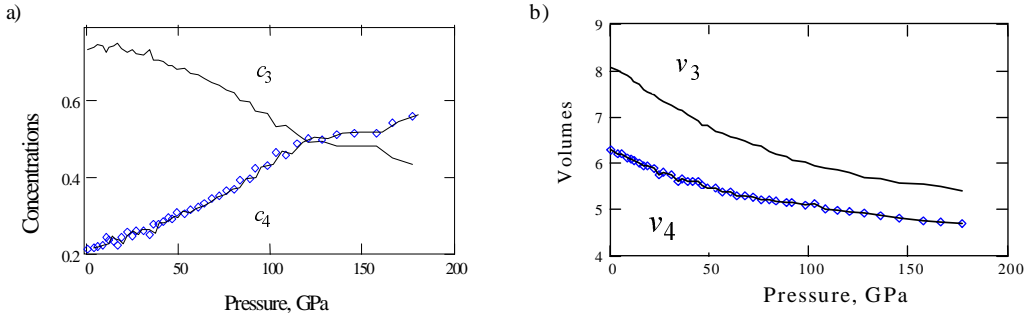


Figure 8: Graphs of (a) concentrations c_3 , c_4 , and (b) volumes v_3 , v_4 as functions of P at $T = 2000$ K.

4 Phase states of a-C

As a result of annealing at $T \geq 1000$ K and $P = 0$ samples of a-C deposited from the atom beam, independently of z in initial state, transforms into state with $z \approx 3.21$ and $\rho \approx 2.61$ g/cm³. In these simulations (CEPS) we have used cells with $N = 776$ and $N = 516$. In the initial states the samples had $z = 3.3 < z^*$, $\rho = 2.62$ g/cm³, and $z = 3.4 > z^*$, $\rho = 3.2$ g/cm³. The annealing times were up to 15 ps. No significant changes of states were recognized at the end of the annealing procedure. The obtained by the annealing metastable state of a-C has properties close to that of GLC ($z < z^*$) formed by beam deposition. The obtained result shows that at $P = 0$, GLC is the equilibrium phase of a-C.

Because in crystalline states along with the stable low pressure phase, graphite, exists also diamond which is stable at high pressure, one could expect that a-C also possesses a phase state which is stable at high pressures. To check this idea we have investigated the states of a-C stabilized at $0 \leq P \leq 200$ GPa and $10^3 \leq T \leq 7 \cdot 10^3$ K.

Two sets of runs were performed. In the first of them the temperature was kept constant. In the second set the pressure was constant. The simulations at constant temperature were performed as following. Prepared by atom beam deposition sample

($z = 3.28$, $\rho = 2.64$ g/cm³) after relaxation at a chosen temperature (1000, 1500, 2000, 2500, 3000 K) was compressed step by step. At each of the steps the linear size of the cell was reduced on 0.05 \AA . Then the sample was equilibrated in thermostat during 6 ps before the next compression step started. One run time was up to 314 ps. A similar procedure was applied in simulations with constant pressure. At all pressures ($P = 1.5, 20, 50, 100, 150$ GPa) initial temperature was chosen to be equal to 2500 K. It increased in successive steps with step width $\Delta T = 100$ K.

As an example, specific volume, average volumes v_3 and v_4 , and z vs. P at $T = 2000$ K are shown on Fig. 8. The pressure dependence of the specific volume is essentially nonlinear (Fig. 8a) due to changes of LO and coordination. Interestingly that compressibilities of v_3 and v_4 both are equal to about 10^{-3} GPa at $P > 100$ GPa what is almost 4 times smaller than those at $P < 10$ GPa. It means that with $z \approx 3.5$ the environments of 3-fold coordinated sites are as rigid as those of the 4-fold coordinated sites. In other words, not coordination but topology of the carbon CRN determines macroscopic properties of a-C.

Results of simulations at constant P are depicted on Fig. 9. Specific volume vs. T is shown on Fig. 9a. It is seen that the compressibility changes dramatically at $P > 50$ GPa, as it took place also at lower temperatures. Besides, the thermal expansion coefficient (it is proportional to slope of $v(t)$) and the heat capacity (slope of the potential energy, E_p , vs T) change considerably in narrow temperature regions which are marked on Fig. 9 by circles. It is naturally to treat the marked temperatures as $T_g(P)$ because not first but second derivatives of the free energy change step-like at the glass transition. The slope dT_g/dP equals about 20 K/GPa. As it is known, T_g depends on the heating and compression rates. In our simulations these rates were varying not so much to recognize this dependence. The results of the investigation of the a-C phase states are summarized on 10 where the levels of constant z on the (P, T) plane are shown. Because the pair correlation lengths are not considerably dependent on (P, T) ,

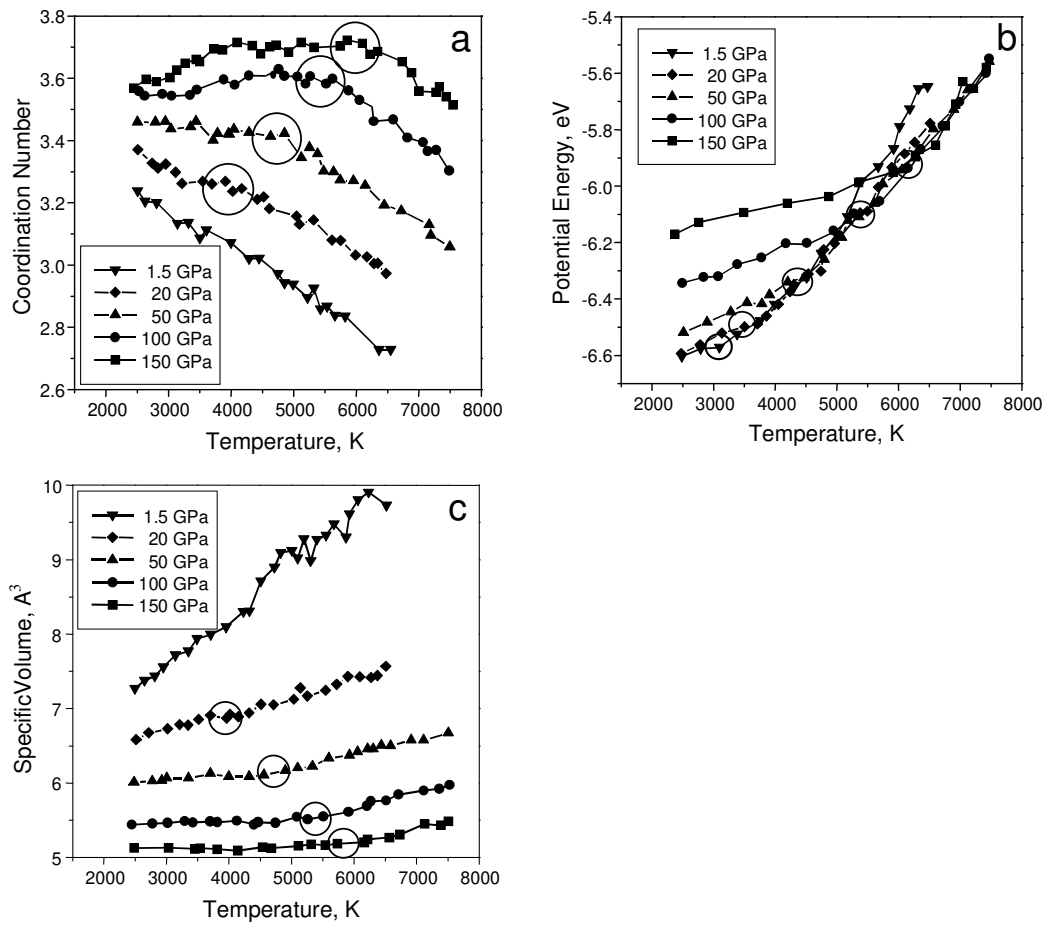


Figure 9: (a) Coordination number, (b) potential energy, and (c) specific volume of a-C as functions of temperature at fixed pressure. Temperature intervals where slopes of the curves are changing are marked by circles

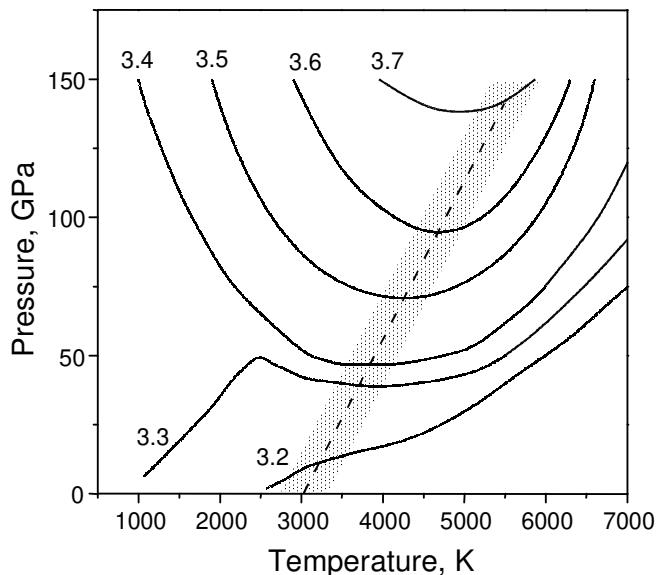


Figure 10: The map of isoconfigurational states (see text). The region of glass-to-liquid transition is shadowed.

the equation

$$z(P, T) = const \quad (8)$$

determines curves of isoconfigurational states.

The performed investigations show that the states with $z \geq 3.4$ have structure and physical properties considerably different from those of states with $z \leq 3.3$. Topologies of the isoconfigurational state curves with $z \geq 3.4$ and $z \leq 3.3$ are also essentially different. Therefore we can conclude that a -C possesses two phase states, GLC and DLC in the used here terminology. The phase diagram of a-C is shown on Fig. 11. The transition region between GLC and DLC is dashed. The glass-to-liquid transition region is also shown. The applied approach do not allow to conclude whether first order phase transition GLC-to-DLC exists or not. It worth noting that continuous phase transformation without phase transition, are also possible, especially in amorphous states [14-17]. This kind of the phase transformation takes place when heterophase fluctuations are strong in the vicinity of the coexisting curve. To solve the problem of the phase transitions of a- C additional investigations have to be done. As it was pointed above, the structure relaxation kinetics is too slow to be essential below $T = 1000$ K. Therefore on the map (10.) this temperature region belongs to the quenched a-C states, (QC), in which appreciable short range reordering is not seen.

5 Concluding remarks

Results of the simulations surprisingly support an old idea on the mechanism of DLC formation under ion beam deposition. In accordance with this idea energetic atom or ion forms small (its size depends on the atom energy) region in which local temperature and pressure are rather high to initiate sp^3 binding formation. If the pressure increases with the energy, E_a , then the concentration c_4 has also to increase. Experimental observations agree with idea. In [18-21] the empiric expressions are proposed and used to estimate $c_4(E_a)$. Evidently the idea of the fast equipartition of kinetic energy in a compact region on the ballistic stage, when a few atoms are involved in collisions, is incorrect. Just on this stage majority of inelastic replacements and displacements, including bonding changes and formation, happen. Afterward some structure relaxation takes place on the short stage of thermalization and quenching. Nevertheless it turns out that in total complicate collisional and thermalization kinetics of the a-C formation by beam deposition looks like result of generation of statistically independent temperature and pressure

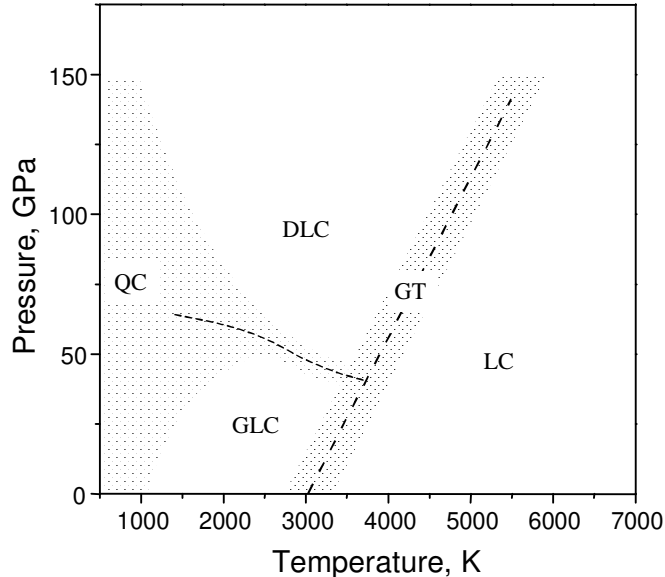


Figure 11: Phase diagram of a-C regions (CEPS results) of the stability, DLC, quenched a-C (QC) and liquid C (LC) are shown. The region of GLC-to-DLC transition and the region of glass-to-liquid transition (GT) are shadowed

microspikes. Let us assume that the structure relaxes toward equilibrium (for the current P and T) state and then this last one occurs quenched. With this assumption it has to be concluded that $P < 50$ GPa at $E_a = 10$ eV, and $P > 50$ GPa with $E_a = 40$ eV with effective temperature 3000...5000 K. In [20] effective pressure was estimated to be about 10 GPa in result of an empiric expression fitting. The collision dynamics of depositing atoms bonding rearrangements was investigated in a density functional based TBMD scheme in [22, 23]. It was found that below $E_a = 30$ eV atoms surface rearrangements dominates. The fraction of sp^3 bonds considerably increases at $E_a \approx 30$ eV when subsurface processes dominate. These results are in qualitative agreement with basic ideas formulated in [18-21], but no molten states were identified in the simulations.

Another evident idea concerns rigidity of a-C. Bulk modulus of graphite is almost twice smaller than that of diamond. For this reason it could be expected that the rigidity of a-C increases rapidly with c_4 above the site percolation threshold which is equal to $c_4^* \approx 0.43$ for diamond-like lattice. In other words, GLC-to-DLC topologic transition takes place at $z = z^* \approx 3.4$ [24]. Moreover the bulk modulus of DLC has to increase as

$$(z - z^*)^\gamma + const, \quad \gamma = 3.3 \quad (9)$$

above the percolation threshold (see [25, 26, 27]). The elastic moduli of a-C above z^* increases very fast (see Fig.2) but the law (9) evidently is out of rule because, as it was shown above, v_3 changes rapidly and rigidities of the sp^2 - and sp^3 -networks in the vicinity z^* are almost equal each to other.

Nevertheless manifestations of the percolation transition of sp^3 -network are considerable in the temperature dependencies of z at $P > 50$ GPa. As it is seen from Fig. 8 and Fig. 9, $z(T)$ is flat or has a positive slope below $T_g(P)$ for the states with $z > 3.4$, i.e. with $z > z^*$. This result can be interpreted as following. Above the percolation threshold the sp^3 -network forms a rigid skeleton which in average have smaller thermal expansion coefficient than that of the sp^2 -network. Therefore fringes of the sp^3 -network play role of compression cell walls for sp^2 bonded atoms. When temperature increases $sp^2 \rightarrow sp^3$ transformations take place due to thermoelastic stresses. Above $T_g(P)$ the skeleton is molten and, as result, average coordination drops. The basic problem of any simulations is to ascertain to which extension a model mimics reality. The same is with used here approaches. Tersoff's version of the potential energy allows correctly simulate graphite and diamond structure at low temperatures. But it is not so good (as it is pointed out i. e. in [28, 29]) for simulations at big T , in the vicinity of T_m and above T_m . For

example, in Tersoff's version of CEPS the diamond melting temperature is equal to 6200 K [30] which is about 1700 K larger than the experimentally determined quantity. Currently we are investigating a-C states taking into account the torsion energy. Boundaries of DLC and GLC occupation regions have to be changed, T_g -curve has to be shifted, but schematically the phase state map of a-C is expected to have a similar scheme. Account of the torsion energy impacts on equilibrium concentrations c_2, c_3, c_4 and, consequently, on topology of the isoconfigurational curves. Determined in [28] T_m of diamond is close to the experimentally measured quantity. It is expected that $T_g(P)$ will be lower than that established in the reported here simulations. This expectation is based on the empirical rule:

$$T_g \approx 2T_m/3 \quad (10)$$

which valid for all glass-forming substances. For example, with $T_m = 6200$ K it has to be $T_g = 4600$ K what is in accord with presented above results.

If topology and connectivity of the sp^3 -network plays a decisive role in GLC-to-DLC transition then the curve

$$c_4(P, T) = c_4^* \quad (11)$$

determines the boundary between GLC and DLC phases on the map of isoconfigurational states. Here c_4^* is the percolation threshold of the sp^3 -network. The equation (11) determines the curve of topologic phase transition. The site probability to belong to the percolation cluster is its order parameter. The topologic phase transition in a-C occurs directly connected with thermodynamic phase transition since c_4 depends on P, T and dynamic, and thermodynamic quantities are sensitive to the CRN topology changes in the vicinity of c_4^* . If an amorphous phase with c_4 exist then phase transition between this phase and a phase with $c_4 \neq 0$ is unavoidable. It is the first order phase transition if c_4 changes step-like across the coexistence curve. Otherwise it is the phase transition of a higher order.

As it was reported in [29] sp^2 -liquid (the liquid with overwhelming 3-fold coordination of atoms) does not exist above the melting point of graphite as it follows from CEPS of carbon in which the torsion energy is taken into account (it is because the torsion energy diminishes entropy of sp^2 bonded structures as compare to sp - and sp^3 -bonding). At lower temperatures role of the entropy in structure formation becomes less important. With that sp^2 -liquid can appear above T_g of GLC. In this case sp^2 -liquid-to- sp -liquid transition exists. Currently hunting of this transition is in progress.

References

- [1] A.S. Bakai and V.E. Strel'nitskij, *Structure and properties of carbon condensates obtained by fast particle flux deposition*, (in Russian), Atominform, Moscow, (1984).
- [2] J. Robertson and E.P. O'Reily, *Phys.Rev. B* **35**, 2946 (1987).
- [3] S. Aisenberg, and F.M. Kimock, *Mater. Sci. Forum* **52**, 1 (1990).
- [4] J. Robertson, *Progr. Solid State Chem.* **2**, 199 (1991).
- [5] P.C. Kelires, *Phys. Rev. B* **47**, 1829 (1993).
- [6] R. Palmer, *Adv. Phys.* **31**, 669 (1982).
- [7] L.S. Palatnik, A.A. Nechitailo and A.A. Koz'ma, *Docl. Akad. Nauk SSSR* **36**, 1134 (1981).
- [8] C.A. Angell, *Science* **267**, 1924 (1995).
- [9] P.W. Anderson, in *Lectures on amorphous systems*, R. Balian (ed.), it III-Condensed Matter, North-Holland, Amsterdam, (1979).
- [10] H.P. Kaukonen and R.M. Nieminen, *Phys. Rev. Lett.* **68**, 620 (1992).
- [11] C. Lee, W. Lambrecht, B. Segal, P. Kelires, Th. Frauenheim and U. Stephan, *Phys.Rev. B* **49**, 1148 (1994).
- [12] Th. Frauenheim, P. Blaudeck, U. Stephan and G. Jungnickel, *Phys. Rev. B* **48**, 4823 (1993).

- [13] N.A. Marks, D.R. Mckenzie, B.A. Pailthorpe, M. Bernasconi and M. Parrinello, *Phys. Rev. B* **54**, 9703 (1996).
- [14] A.S. Bakai, *Low Temp. Phys.* **22**, 733 (1996).
- [15] A.S. Bakai, *Low Temp. Phys.* **24**, 20 (1998).
- [16] E.W. Fischer and A.S. Bakai, in *Slow dynamics in complex systems*, M. Tokuyama and I. Oppenheim (eds.), AIP Conf. Proc. 1999, **469**, 325 (1999).
- [17] A.S. Bakai, *Condensed Matter Phys.* **3**, 675 (2000).
- [18] J. Robertson, *Diamond Relat. Mater.* **2**, 984 (1993).
- [19] C.A. Davis, *Thin Solid Films* **226**, 30 (1993).
- [20] P.J. Fallon, V.S. Veerasamy, C.A. Davis, et. al., *Phys. Rev. B* **48**, 4777 (1993).
- [21] Y. Lifshitz, S.R. Kasi and J.W. Rabalais, *Mater. Sci. Forum* **52-53**, 237 (1990).
- [22] S. Uhlmann, Th. Frauenheim and U. Stephan, *Phys. Rev. B* **51**, 4541 (1995).
- [23] S. Uhlmann, Th. Frauenheim and S. Lifshitz, *Phys. Rev. Lett.* **81**, 641 (1998).
- [24] D. Stauffer, *Introduction to percolation theory*, Tailor & Francis Ltd. (1985).
- [25] Y.Kantor and I. Webman, *Phys. Rev. Lett.* **52**, 1891 (1984).
- [26] D. Bergman, *Phys. Rev. B* **31**, 1696 (1982).
- [27] A.S. Bakai, V.Yu. Gonchar, S.V. Krikun and G.Ya. Lubarsky, *Functional materials* **2**, 222 (1995).
- [28] N.J. Glosli and F.H. Ree, *J.Chem. Phys.* **110**, 441 (1999).
- [29] N.J. Glosli and F.H. Ree, *Phys. Rev. Lett.* **82**, 4659 (1999).
- [30] J.Tersoff, *Phys. Rev. Lett.* **61**, 2879 (1988).